Advanced Mathematical Models & Applications
Vol.5, No.1, 2020, pp.80-94

Jomard Publishing

A COMPARATIVE STUDY BETWEEN TV, TV^2, BTV AND COMBINED MODELS FOR THE MULTI-FRAME SUPER-RESOLUTION

Amine Laghrib*

Sultan Moulay Slimane University, Meghila, Beni-Mellal, Morocco

Abstract. Variational models are considered as successful methods for image processing and analysis, especially in the case of the super-resolution algorithms. In this paper, we present some comparisons between the Total Variation (TV) and other high-order variational models and provide detailed discretization of these models and numerical implementation for solving these models. We demonstrate the advantages and disadvantages between these models in the context of super-resolution through many experiments. The methods and techniques can also be used for other applications, such as image segmentation, dehazing and illumination reduction.

Keywords: image denoising, super-resolution, restoration step, total variation.
AMS Subject Classification: 65J22, 65F22, 68U10.
Corresponding author: Amine Laghrib, Sultan Moulay Slimane University, Meghila, Beni-Mellal, Morocco, e-mail: *a.laghrib@usms.ma*
Received: 6 January 2020; Revised: 2 February 2020; Accepted: 25 March 2020; Published: 29 April 2020.

1 Introduction

Image super resolution (SR) reconstruction is a challenging problem in image processing. The principle of this technique is to build a high-resolution (HR) image by fusing and restoring degraded low-resolution (LR) ones. The SR is used in many applications, such as MRI images, video surveillance and satellite imaging.

Several techniques of the muliframe SR have been proposed to enhance the quality of the obtained HR image with different success degrees (El Mourabit et al., 2017; Laghrib et al., 2016, 2018a, 2017, 2019a). To reduce the complexity of the SR approaches, it is decomposed into two steps: first, finding a blurred HR image from the LR measurements, then, deblurring and denoising it. Both steps are critical to the quality of the HR image. We concentrate here on the second one; we impose some prior on the HR image in a Bayesien framework. Some of the widely-used prior functions are Total Variation (TV)-type regularizers (Rudin et al., 1992; Caselles et al., 2015; Laghrib et al., 2019b). Another successful regularization is the bilateral total variation (BTV) with the L^1 norm proposed by Farsiu et al. (2004). These approaches are successful in recovering images with sharp edges but fail on images with smooth surface, suffering from the staircasing effect. To overcome this defect, high-order variational approaches (Chan et al., 2000; Bergounioux & Piffet, 2010; Chambolle & Lions, 1997) can be used. Despite its success in numerous denoising problems, it suffers from blur effect. To perform the process of simultaneous deblurring and denoising, a combined first and second order regularization have been performed (Chambolle & Lions, 1997; Gottlieb et al., 2001; Papafitsoros & Schönlieb, 2014) has been used and proved its robustness in image restoration. In the super-resolution context, two combined high-order models have been introduced, such as: the combined TV and BTV regularizations (Laghrib et al., 2015) and the combined TV^2 and BTV regularizations (Laghrib et al., 2018b).

In the following, we present a comparative study between the above high-order and TV models in the context of the super-resolution.

2 Problem formulation

The observed images of a real scene are usually in low resolution due to some degradation operators. In practice, the acquired image is corrupted by noise, blur and sampling. We assume that the LR images are taken under the same environmental conditions using the same sensor. The relationship between an ideal HR image X of size $M = rN_1 \times rN_2$ denoted by a column vector $X = [x_1, x_2 \ldots, x_M]^\top$, where $r \geq 1$ is the downsampling factor and the LR images Y_k of size $N_1 \times N_2$, represented also by a column vector $Y_k = [y_{k,1}, y_{k,2} \ldots, y_{k,N_1N_2}]^\top$, where $k = 1 \ldots n$ and n is the number of the LR images, is given by the relation

$$Y_k = DF_kHX + e_k, \qquad \forall k = 1, 2, \ldots, n, \tag{1}$$

where H represents the linear blur operator of kernel size $M \times M$, D represents the sampling operator of size $N_1N_2 \times M$, F_k is a geometric warp matrix of size $M \times M$ representing a non-parametric transformation that differs in all frames, and e_k a vector of size N_1N_2 represents the additive noise for each image, assumed to follow a zero mean Gaussian distribution.

In the presence of different operators of degradation (sampling, blur and noise), the problem becomes very unstable. To deal with it, we use the same approach as in Farsiu et al. (2004) that suggests to separate it into three steps:

1. Computing the warp matrix F_k for each image.

2. Fusing the low-resolution images Y_k into a blurred HR version $B = HX$.

3. Finding the estimation of the HR image X from B.

To compute the warp matrix F_k, there are many approaches in the literature, we use here a non parametric registration (Laghrib et al., 2016). For the fusion step, we use the technique of Farsiu et al. (2004), recalled in the following section.

2.1 The fusion step

The first part of our algorithm is to compute the blurred HR version $B = HX$. We assume that the additive noise is Gaussian distributed and follows the same distribution for all low resolution images. The blurred image $\widehat{B}$ can be found via the principle of maximum likelihood estimator (ML). The ML suggests the choice of $\widehat{B}$ that maximizes the likelihood function, which also minimizes the negative log-likelihood function

$$\begin{aligned} \widehat{B} &= \arg\max_B \{p(Y_k|B)\} \\ &= \arg\min_B \{-\log(p(Y_k|B))\} \\ &= \arg\min_B \sum_{k=1}^{n} \|Y_k - DF_kB\|_{L^2}^2. \end{aligned} \tag{2}$$

The steepest descent algorithm or other optimization methods can be used to resolve this minimization problem.

2.2 Deconvolution and denoising step

In this step we try to find the HR image X by deblurring and denoising the image $\widehat{B}$. Unfortunately we are facing an unstable inverse problem due to the presence of noise and blur at the same time. To overcome this difficulty, we impose some prior knowledge about the image in a Bayesian framework. Since $\widehat{B}$ has white Gaussian noise, the measured vectors Y_k also undergo a Gaussian blur. Via the Bayes rule, finding the HR image X leads us to look for the solution of the following minimization problem (3) using the maximum a posteriori (MAP) estimator

$$\begin{aligned}\widehat{X}_{MAP} &= \arg\max_X\{p(X|\widehat{B})\}\\ &= \arg\max_X\left\{\frac{p(\widehat{B}|X)p(X)}{p(\widehat{B})}\right\}\\ &= \arg\min_X\left\{-\log(p(\widehat{B}|X)) - \log(p(X))\right\},\end{aligned} \tag{3}$$

where $p(\widehat{B}|X)$ represents the likelihood term (data attachment term) and $p(X)$ denotes the prior knowledge on the HR image. To formulate precisely this problem, we need to assume a prior Gibbs function (PGF). This is the role of the regularization term.

2.3 The prior Gibbs function

A well-known manner to represent the image prior PGF function p is the Gibbs function represented by

$$p(X) = c_G \cdot \exp\{-G(X)\}, \tag{4}$$

where c_G is a normalization constant and G is a non negative energy function. In the following, we will see four choice of this function and we will make some comparison results.

3 Total variation regularization (TV)

The main advantage of using the TV regularization is the use of a convex function with respect to the variable X, to stop the isotropic lissage behavior near edges (Rudin et al., 1992). For the super-resolution restoration part, this problem is formulated such as

$$p(X) = \alpha \exp\{-\|\nabla X\|_1\}. \tag{5}$$

To show the existence of the solution to this minimization problem, we use the classical variational calculus based on the relaxation method on the space of bounded variation $BV(\Omega)$ (see Aubert & Kornprobst (2006) for more details on the proof).

The discretization is an essential step in solution of the obtained minimization problem. We give here some notations, we note $X_{i,j}$, $i = 1, ...N,\ j = 1, ..., M$: the discrete image, $\mathcal{X} = \mathbb{R}^{N\times M}$: the set of discrete image of size $N \times M$ et $\mathcal{Y} = \mathcal{X} \times X$.

The spaces $\mathcal{X}$ and $\mathcal{Y}$ are endowed by the scalar products $< .,. >_{\mathcal{X}}$ and $< .,. >_{\mathcal{Y}}$, where

$$\forall X, Y \in \mathcal{X},\ < X, Y >_{\mathcal{X}} = \sum_{i=1}^{N}\sum_{j=1}^{M} X_{i,j}Y_{i,j},$$

and

$$\forall p = (p^1, p^2), q = (q^1, q^2) \in \mathcal{Y},\ < p, q >_{\mathcal{Y}} = \sum_{i=1}^{N}\sum_{j=1}^{M} p^1_{i,j}q^1_{i,j} + p^2_{i,j}q^2_{i,j}.$$

the gradient vector of X noted ∇X defined in $\mathcal{Y}$ such as $\nabla X = ((\nabla X)^1, (\nabla X)^2)$, where

$$(\nabla X)^1_{i,j} = \begin{cases} X_{i+1,j} - X_{i,j} & \text{if } i < N \\ 0 & \text{if } i = N \end{cases}, \quad (\nabla X)^2_{i,j} = \begin{cases} X_{i,j+1} - X_{i,j} & \text{if } j < M \\ 0 & \text{if } j = M \end{cases}. \tag{6}$$

The adjoint operator associated to $-\nabla$ is defined by div : $\mathcal{X}^2 \to \mathcal{X}$ such as $p = (p^1, p^2) \in \mathcal{X}^2$, we have

$$\forall w \in \mathcal{X}, < \text{div } p, w >= - < p, \nabla w > .$$

Then

$$(\text{div } p)_{i,j} = (\text{div } p)^1_{i,j} + (\text{div } p)^2_{i,j}, \tag{7}$$

where

$$(\text{div } p)^1_{i,j} = \begin{cases} p^1_{i,j} - p^1_{i-1,j} & \text{if } 1 < i < N \\ p^1_{i,j} & \text{if } i = 1 \\ -p^1_{i-1,j} & \text{if } i = N \end{cases}, (\text{div } p)^2_{i,j} = \begin{cases} p^2_{i,j} - p^2_{i,j-1} & \text{if } 1 < i < M \\ p^2_{i,j} & \text{if } i = 1 \\ -p^2_{i,j-1} & \text{if } i = M \end{cases}.$$

the discretized version of the TV term, represented by J, is defined such as

$$J(X) = \sum_{i=1}^{N} \sum_{j=1}^{M} |(\nabla X)_{i,j}|,$$

where $|\,.\,|$ is the Euclidean norm of $\mathbb{R}^2$, defined such as

$$|(\nabla X)_{i,j}| = |\left((\nabla X)^1_{i,j}, (\nabla X)^2_{i,j}\right)| = \sqrt{\left(\nabla X)^1_{i,j}\right)^2 + \left((\nabla X)^2_{i,j}\right)^2}$$

To resolve the TV minimization problem, many algorithms have been proposed. In this paper, we choose the Primal-dual (Chambolle & Pock, 2011) algorithm.

4 Second order Total Variation (TV^2)

The main purpose to take the high-order TV is to smooth the regular part of the image and avoiding the starcasing effect, keeping safe as possible the image contours. The associated Gibbs function of the associated super-resolution problem is given by

$$p(X) = \exp\left\{-\delta \|\nabla^2 X\|_1\right\}.$$

In the same way as for the regularization TV, it is necessary first of all to make sure of the existence of solution. This done also by the relaxation techniques (see Aubert & Kornprobst (2006)).

For the discretization step we will need some to define some operators discretized such as the second order operator, noted ∇^2

$$\nabla^2 X = \begin{pmatrix} \nabla_{xx} X & \nabla_{xy} X & \nabla_{xy} X & \nabla_{yy} X \end{pmatrix},$$

where

$$\nabla_{xx} X_{i,j} = \begin{cases} X_{i,M_2} - 2X_{i,1} + X_{i,2} & \text{if } 1 \le i \le M_1,\ j = 1, \\ X_{i,j-1} - 2X_{i,j} + X_{i,j+1} & \text{if } 1 \le i \le M_1,\ 1 < j < M_2, \\ X_{i,M_2-1} - 2X_{i,M_2} + X_{i,1} & \text{if } 1 \le i \le M_1,\ j = M_2, \end{cases}$$

$$\nabla_{yy}X_{i,j} = \begin{cases} X_{M_1,j} - 2X_{1,j} + X_{2,j} & \text{if } i = 1,\ 1 \le j \le M_2, \\ X_{i-1,j} - 2X_{i,j} + X_{i+1,j} & \text{if } 1 < i < M_1,\ 1 \le j \le M_2, \\ X_{M_1-1,j} - 2X_{M_1,j} + X_{1,i} & \text{if } i = M_1,\ 1 \le j \le M_2, \end{cases}$$

on the other part, we have

$$\nabla_{xy}X_{i,j} = \begin{cases} X_{i,j} - X_{i+1,j} - X_{i,j+1} + X_{i+1,j+1} & \text{if } 1 \le i < M_1,\ 1 \le j < M_2, \\ X_{i,M_2} - X_{i+1,M_2} - X_{i,1} + X_{i+1,1} & \text{if } 1 \le i < M_1,\ j = M_2, \\ X_{M_1,j} - X_{1,j} - X_{M_1,j+1} + X_{1,j+1} & \text{if } i = M_1,\ 1 \le j < M_2, \\ X_{M_1,M_2} - X_{1,M_2} - X_{M_1,1} + X_{1,1} & \text{if } i = M_1,\ j = M_2. \end{cases}$$

In addition, for $X = (X_1,\ X_2,\ X_3,\ X_4) \in \left(\mathbb{R}^M\right)^4$, we define the operator div^2 such as

$$(\mathrm{div}^2 X)_{i,j} = \overline{\nabla_{xx}}X_{1_{i,j}} + \overline{\nabla_{yy}}X_{2_{i,j}} + \overline{\nabla_{xy}}X_{3_{i,j}} + \overline{\nabla_{xy}}X_{4_{i,j}},$$

where

$$\overline{\nabla_{xx}} = \nabla_{xx},\ \overline{\nabla_{yy}} = \nabla_{yy},$$

and

$$\overline{\nabla_{xy}}X_{i,j} = \begin{cases} X_{1,1} - X_{1,M_2} - X_{M_1,1} + X_{M_1,M_2} & \text{if } i = 1,\ j = 1, \\ X_{1,j} - X_{1,j-1} - X_{M_1,j} + X_{M_1,j-1} & \text{if } i = 1,\ 1 < j \le M_2, \\ X_{i,1} - X_{i-1,M_2} - X_{i-1,1} + X_{i-1,M_2} & \text{if } 1 < i \le M_1,\ j = 1, \\ X_{i,j} - X_{i,j-1} - X_{i-1,j} + X_{i-1,j-1} & \text{if } 1 < i \le M_1,\ 1 < j \le M_2. \end{cases}$$

To resolve this problem, we use the Primal-dual algorithm (Chambolle & Pock, 2011).

5 Combined TV and TV^2 model

The combined TV and TV^2 model has been introduced in many image processing task to make some balance between the staircasing avoidance and the preservation of the edges. The associated Gibbs function is defined such as

$$P(X) = \exp\left\{-\delta\|\nabla X\|_1\right\} \cdot \exp\left\{-(1-\delta)\|\nabla^2 X\|_1\right\}, \tag{8}$$

where δ is a positive parameter used the control the balance between these two terms. For the discretization of this problem it is simple since we have already discretized the two terms TV and TV^2 previously. We also use the Primal-dual algorithm (Chambolle & Pock, 2011) to resolve this problem.

6 The combined TV and BTV regularization

Based on the strong and weak points of the regularizations treated above, Laghrib et al. (2015) have proposed to combine the regularization TV with the BTV term in the deconvolution and denoising part of the super-resolution. The main idea behind this combination is to regularize with a fairly large weight γ, in the term TV, in order to preserve the essential characteristics of the reconstructed image, such as corners and contours, as best as possible. On the other hand, the use of a small step δ for the term BTV preserves the smooth contours and avoids the appearance of artifacts caused by the regularization TV. Thus, for the choice of the á priori term, the Gibbs function is presented as follows

$$p(X) = \exp\left(-\gamma|||\nabla X|||_1 - \delta \sum_{i=-p}^{p}\sum_{j=-p}^{p} \alpha^{|i|+|j|}||X - S_x^i S_y^j X||_1\right). \tag{9}$$

This problem have been studied in Laghrib et al. (2015) with existence of the solution theorem and comparative study with competitive super-resolution approaches.

7 Combined TV^2 and BTV model

The main idea behind this combination is to use a large weight for the BTV regularization to enhance sharp edges and also to correct the misregistration errors, and use the second order regularizer to eliminate the staircasing caused by the BTV regularization without blurring the image. The existence of a minimizer for this problem (second step of SR), which is a combination of the BTV and second order variational regularization (see Laghrib et al. (2018b) for more details).

$$p(X) = \exp\left\{-\delta \sum_{i=-p}^{p}\sum_{j=-p}^{p} \alpha^{|i|+|j|}\|X - S_x^i S_y^j X\|_1\right\} \cdot \exp\left\{-(1-\delta)\|\nabla^2 X\|_1\right\},$$

where the operators S_x^i and S_y^j shift X by i and j pixels in horizontal and vertical directions respectively

$$S_x^i X(x,y) = X(x+i,y) \text{ and } S_y^j X(x,y) = X(x,y+j).$$

This formulation depends on the following parameters

- α: a scalar weight, applied to give a spatially decaying effect to the summation of the regularization terms, $0 < \alpha < 1$.
- p: the spatial window size, $p \geq 1$.
- δ: the weight that controls the regularization combination. We define in the following how it is calculated from the gradient of the image. This parameter can be computed using learning techniques Lyaqini et al. (2020).

The first term is a measure of bilateral variation, containing a spatial decaying influence and a color difference in the neighborhood. The solution of this problem is performed using the Primal-dual algorithm.

8 Numerical Result

We propose here to compare the models $TV + BTV$ (Laghrib et al., 2015) and $BTV + TV^2$ (Laghrib et al., 2018b) with bicubic interpolation, the TV regularization Rudin et al. (1992), BTV Farsiu et al. (2004), TV^2 Bergounioux & Piffet (2010), and also the combination between the regularizations TV and TV^2 ($TV + TV^2$) Papafitsoros & Schönlieb (2014). To measure the performance of these methods, we construct 40 low-resolution (LR) images with a Gaussian kernel blur of standard deviation $\sigma = 3.5$ and a decimation factor $r = 4$. To measure the robustness of these methods with respect to noise, we add a Gaussian noise with standard deviation $\sigma_{noise} = 10$ to all the LR constructed images. We represent the reconstructed images by the different methods in the figures (1 to 12).

By a visual evaluation, we can deduce the effectiveness of the $BTV+TV^2$ model to eliminate the artifacts. Note that we choose the regularization parameters, depending on the visually pleasing result with the best $PSNR$ in all experiments for the other methods.

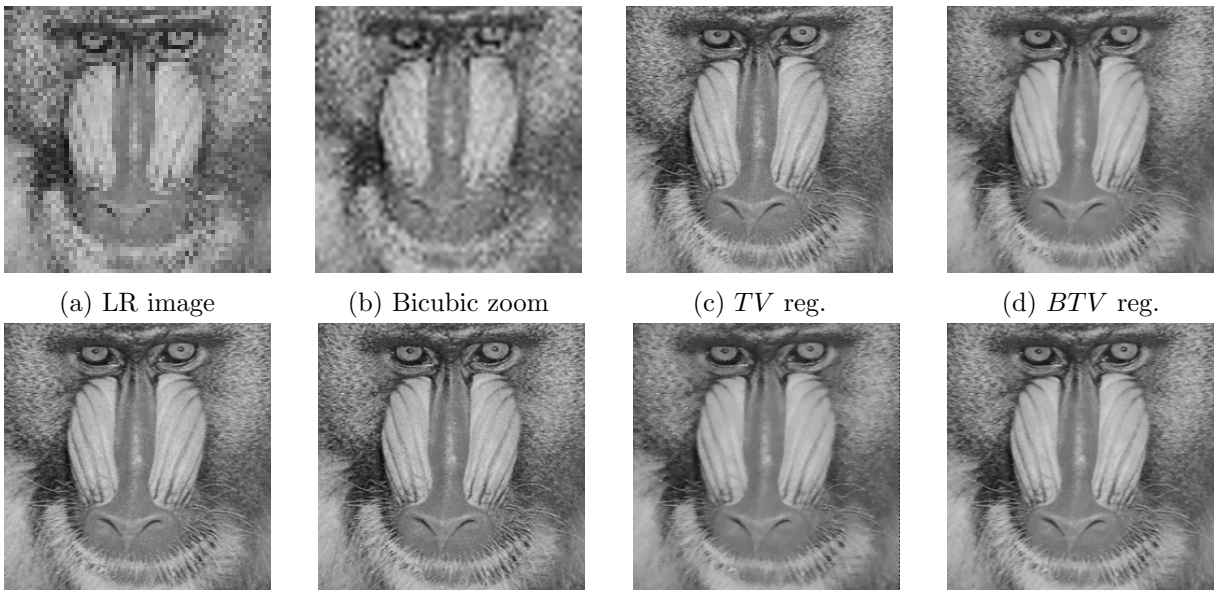

(a) LR image (b) Bicubic zoom (c) TV reg. (d) BTV reg.

(e) TV^2 reg. (f) $TV + TV^2$ reg. (g) $TV + BTV$ (h) $BTV + TV^2$

Figure 1: The image super-resolution of the *Baboon* image using the TV and high-order regularizations.

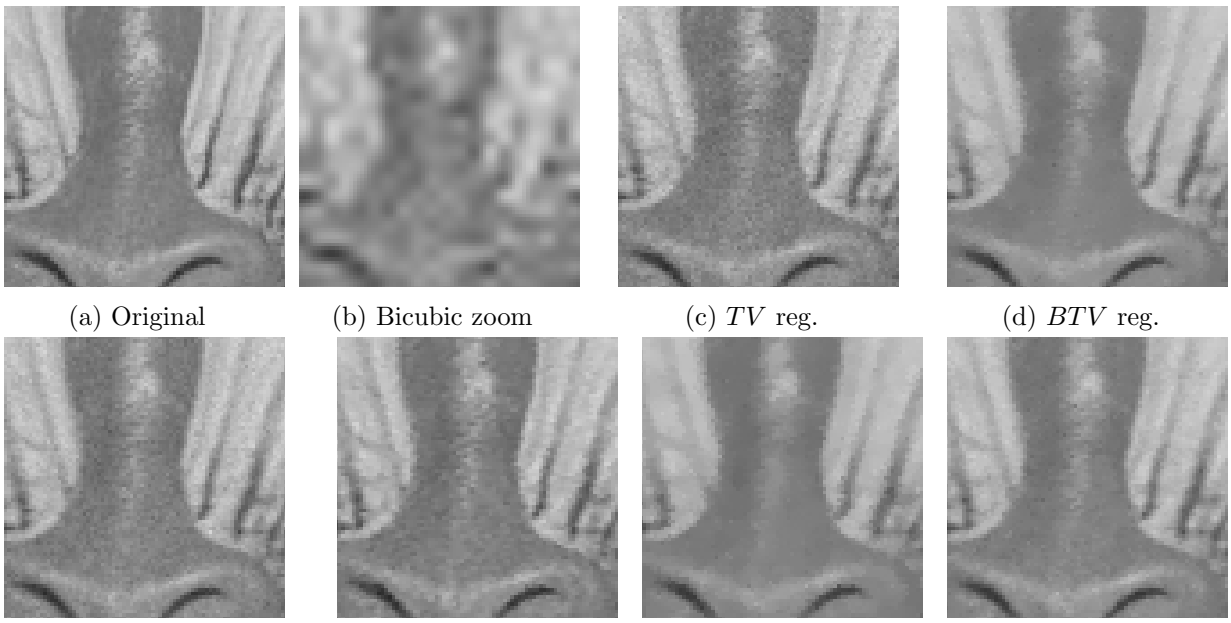

(a) Original (b) Bicubic zoom (c) TV reg. (d) BTV reg.

(e) TV^2 reg. (f) $TV + TV^2$ reg. (g) $TV + BTV$ (h) $BTV + TV^2$

Figure 2: Zoom on a part of the obtained result in the previous test of *Baboon* image. We observe that the staircasing effect is almost suppressed in the image obtained by the $BTV+TV^2$ method when compared with the other methods. We can also see that the models $TV + TV^2$ and the $TV + BTV$ models suppress the staircasing effect, but do not preserve enough the contours and the details of the image. On the other hand, it is interesting to see that the $BTV + TV^2$ model behaves like the BTV model in areas with more details like the nose of the Baboon and like the TV^2 model elsewhere.

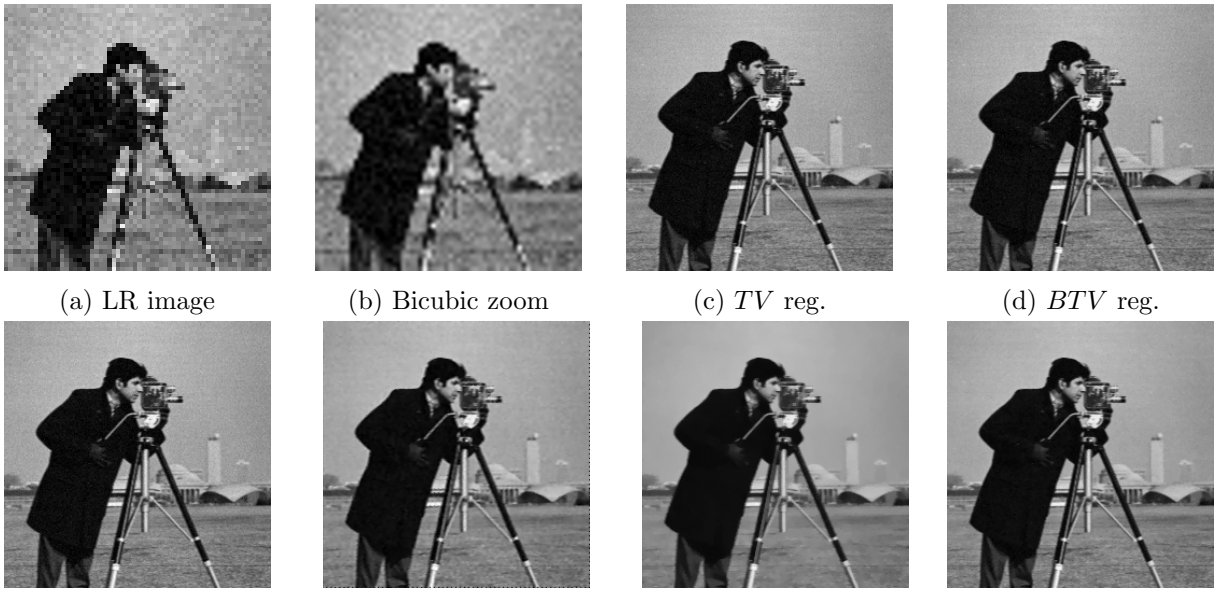

(a) LR image (b) Bicubic zoom (c) TV reg. (d) BTV reg.

(e) TV^2 reg. (f) $TV + TV^2$ reg. (g) $TV + BTV$ (h) $BTV + TV^2$

Figure 3: The super-resolution of the LR sequence of *Cameraman* image using differents regularizations.

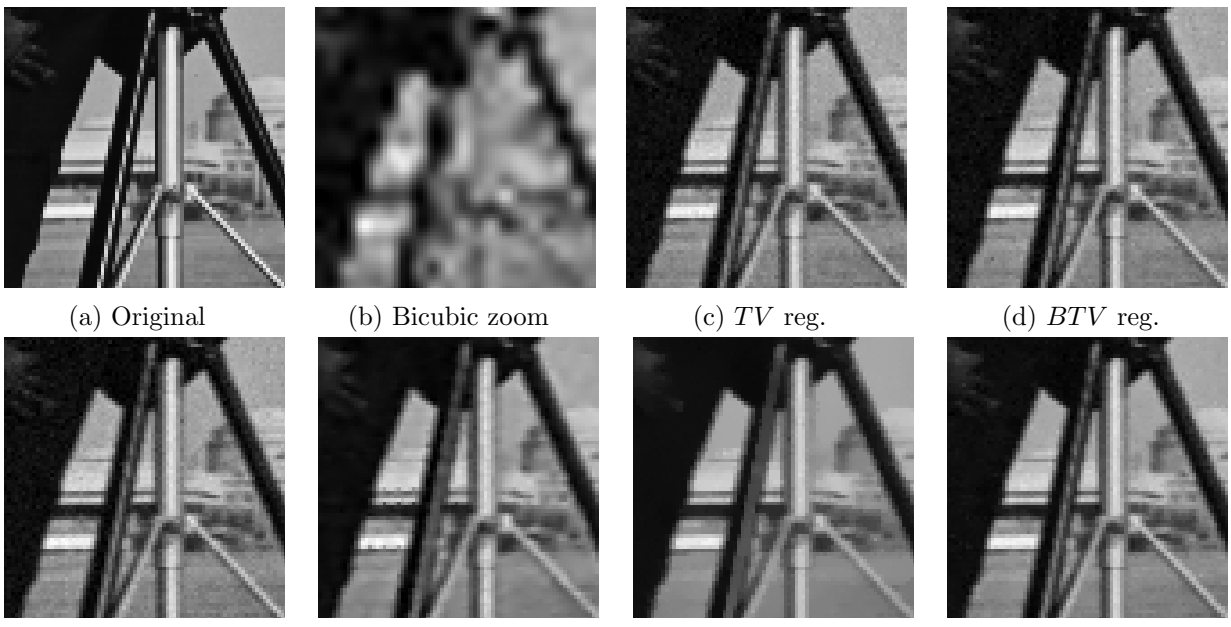

(a) Original (b) Bicubic zoom (c) TV reg. (d) BTV reg.

(e) TV^2 reg. (f) $TV + TV^2$ reg. (g) $TV + BTV$ (h) $BTV + TV^2$

Figure 4: Zoom on a part of the obtained results in the previous Figure compared to the original image of *Cameraman*. We can observe the same thing as the previous test. 2.

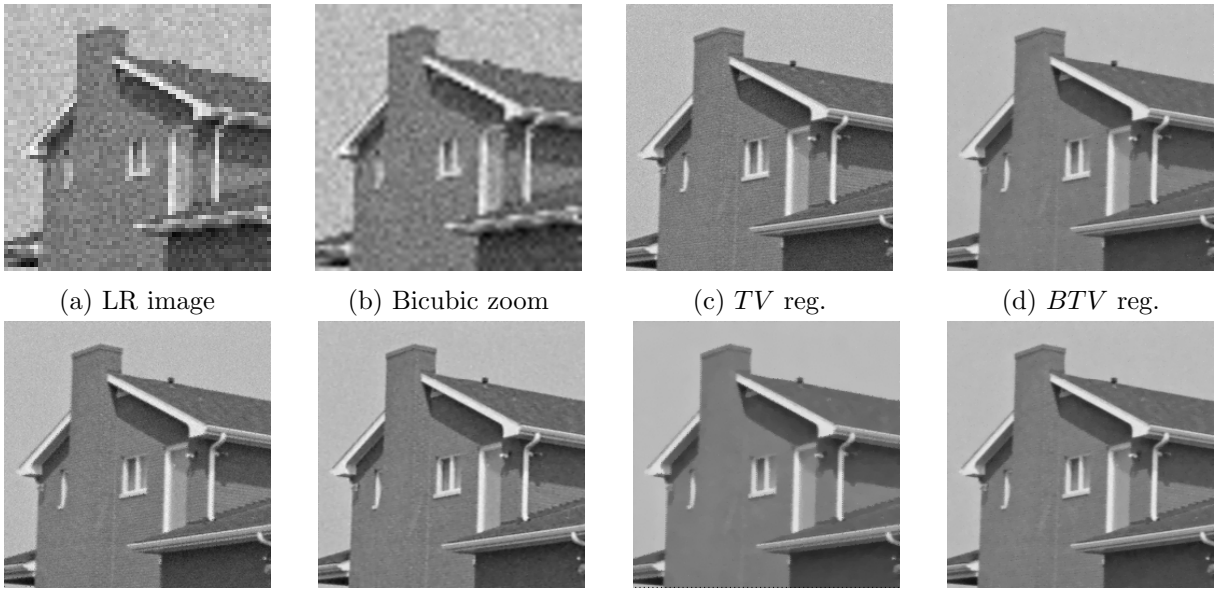

(a) LR image (b) Bicubic zoom (c) TV reg. (d) BTV reg.

(e) TV^2 reg. (f) $TV + TV^2$ reg. (g) $TV + BTV$ (h) $BTV + TV^2$

Figure 5: The super-resolution result of the *House* image using different regularization terms.

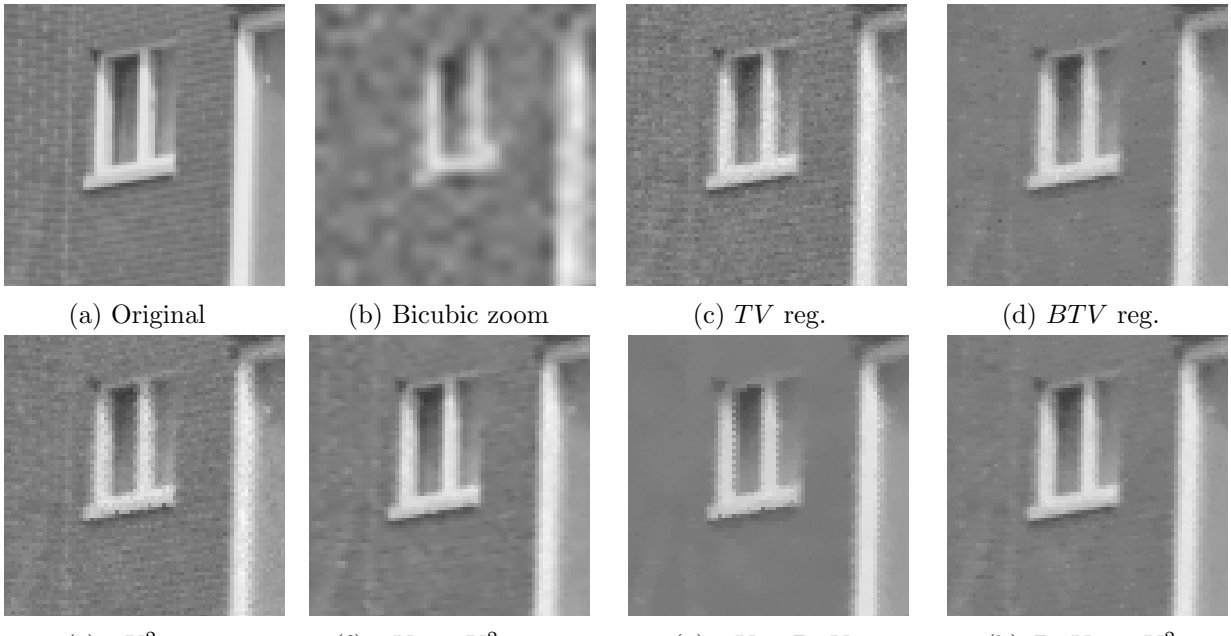

(a) Original (b) Bicubic zoom (c) TV reg. (d) BTV reg.

(e) TV^2 reg. (f) $TV + TV^2$ reg. (g) $TV + BTV$ (h) $BTV + TV^2$

Figure 6: Zoom on a part of the *House* image obtained using different regularization terms. We can observe that the two models $TV + TV^2$ and $BTV + TV^2$ supress the noise while the texture is preserved compared to other models.

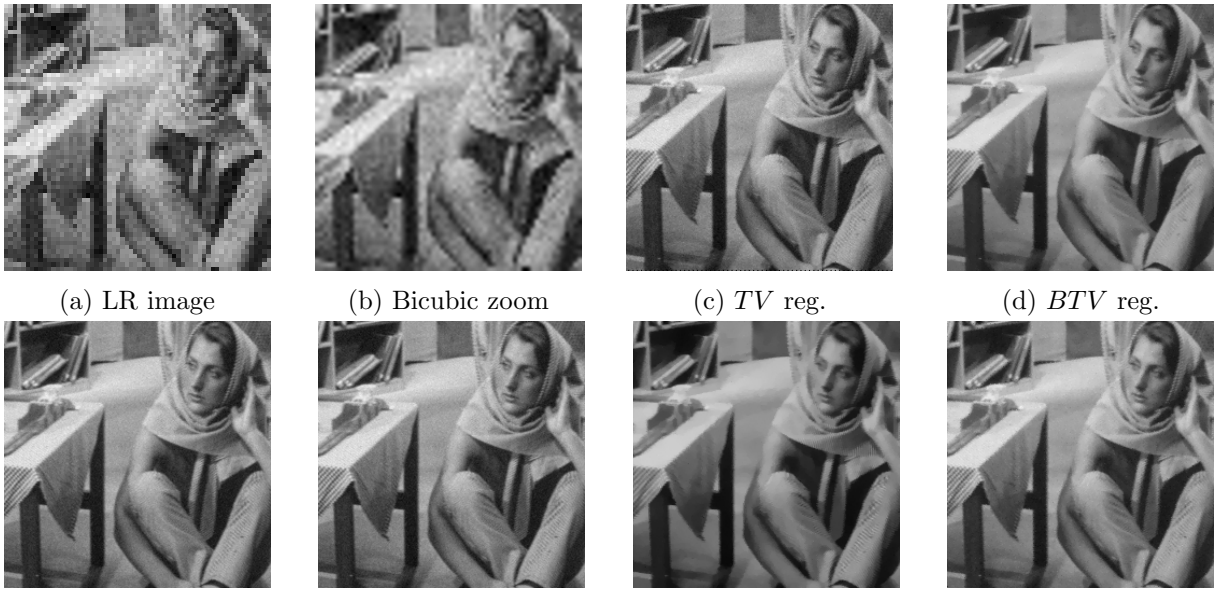

(a) LR image (b) Bicubic zoom (c) TV reg. (d) BTV reg.

(e) TV^2 reg. (f) $TV + TV^2$ reg. (g) $TV + BTV$ (h) $BTV + TV^2$

Figure 7: The obtained super-resolution results of the *Barbara* image using different SR regularizations.

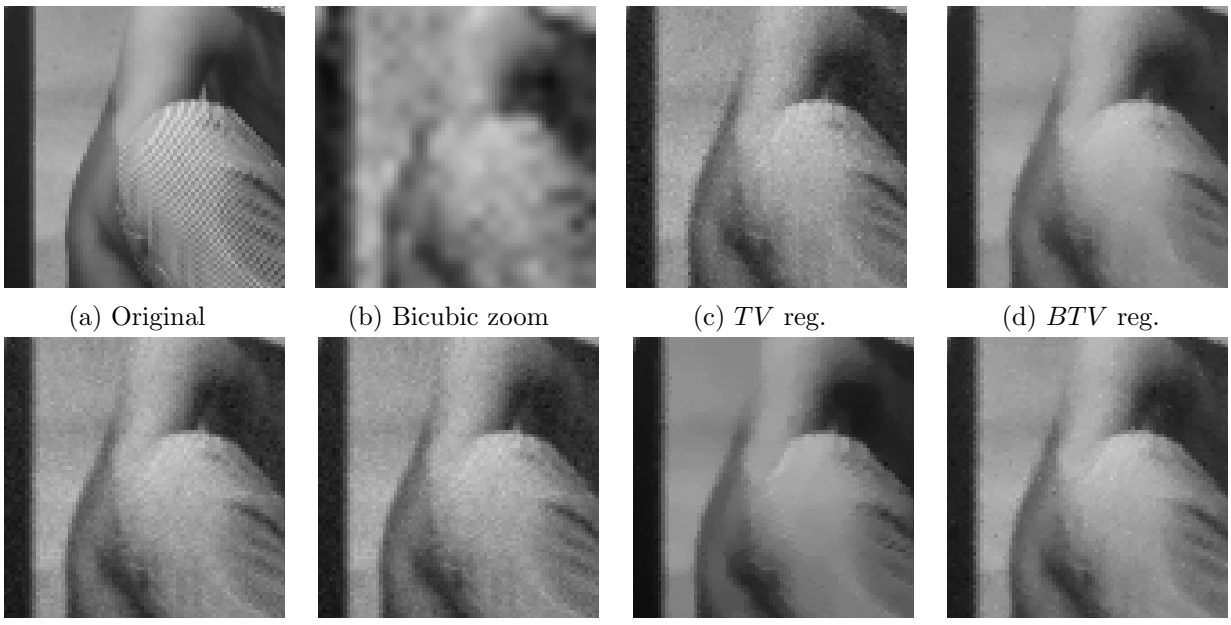

(a) Original (b) Bicubic zoom (c) TV reg. (d) BTV reg.

(e) TV^2 reg. (f) $TV + TV^2$ reg. (g) $TV + BTV$ (h) $BTV + TV^2$

Figure 8: Zoom on a part of the *Barbara* image obtained using different regularizations SR. We can detect that the staircasing effect is less in the obtained image by the $BTV + TV^2$ regularization, compared to other models.

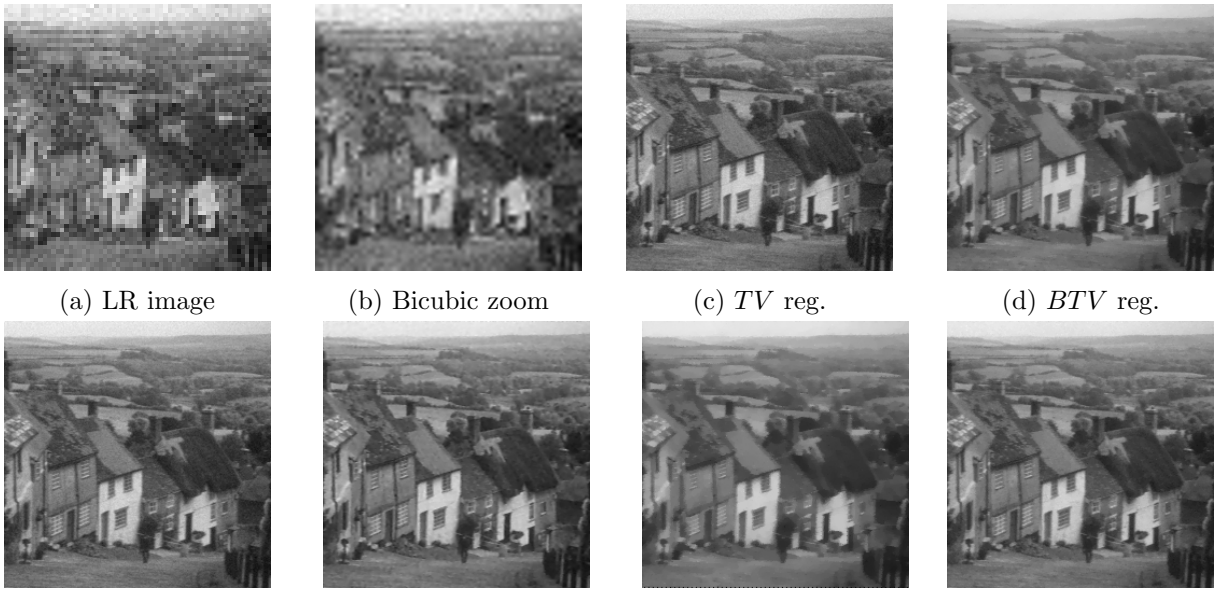

(a) LR image (b) Bicubic zoom (c) TV reg. (d) BTV reg.

(e) TV^2 reg. (f) $TV + TV^2$ reg. (g) $TV + BTV$ (h) $BTV + TV^2$

Figure 9: The super-resolution method of the *Goldhill* image using different regularization terms.

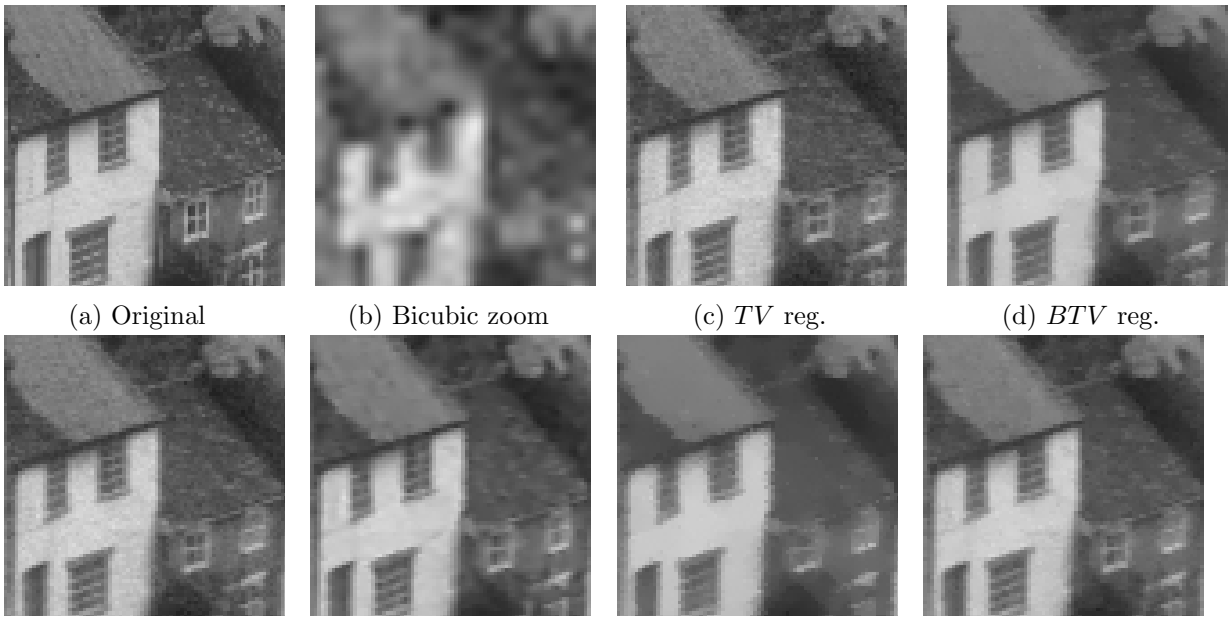

(a) Original (b) Bicubic zoom (c) TV reg. (d) BTV reg.

(e) TV^2 reg. (f) $TV + TV^2$ reg. (g) $TV + BTV$ (h) $BTV + TV^2$

Figure 10: Zoom on a part of the super-resolved *Goldhill* image.

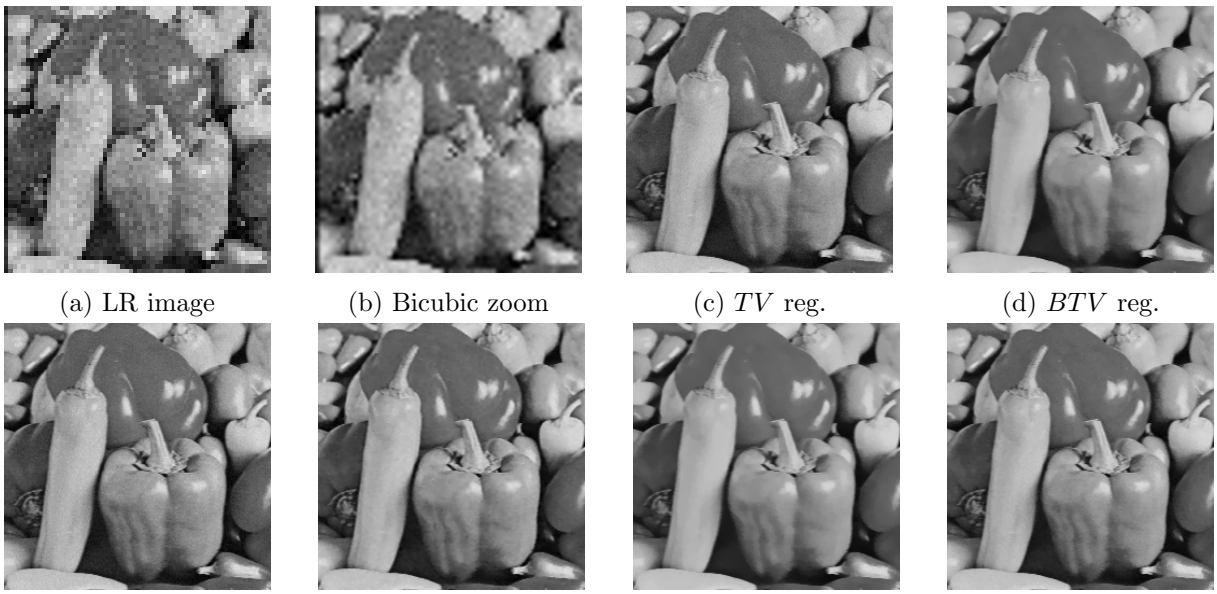

(a) LR image (b) Bicubic zoom (c) TV reg. (d) BTV reg.

(e) TV^2 reg. (f) $TV + TV^2$ reg. (g) $TV + BTV$ (h) $BTV + TV^2$

Figure 11: The super-resolution result of the *Peppers* image using different regularizations.

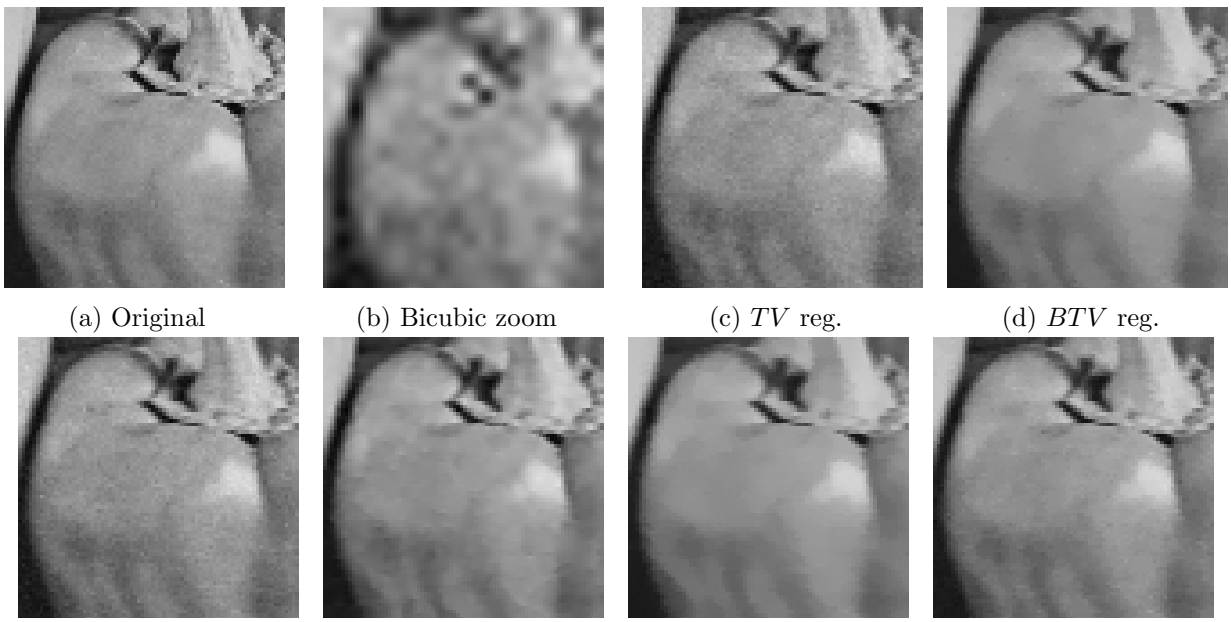

(a) Original (b) Bicubic zoom (c) TV reg. (d) BTV reg.

(e) TV^2 reg. (f) $TV + TV^2$ reg. (g) $TV + BTV$ (h) $BTV + TV^2$

Figure 12: Zoom on a part of the super-resolved *Peppers* image.

Table 1: The obtained $PSNR$ and $SSIM$ results using different regularization terms and different σ noise. In *bold* number the best and higher score in each row.

Image			Method						
	σ bruit	Mesure	Bicubic	TV	second ordre	BTV	$TV+TV^2$	$BTV+TV$	$TV+TV^2$
Baboun	10	PSNR	22.47	29.16	29.42	29.28	29.59	29.964	**30.29**
		SSIM	0.429	0.860	0.866	0.868	0.867	0.810	**0.870**
	15	PSNR	19.94	28.02	28.57	28.75	28.69	29.33	**29.74**
		SSIM	0.363	0.797	0.791	0.813	0.821	0.807	**0.832**
Cameraman	10	PSNR	21.92	28.46	28.32	28.92	28.66	28.63	**29.03**
		SSIM	0.578	0.790	0.775	0.857	0.864	0.870	**0.890**
	15	PSNR	20.67	27.17	27.49	28.01	27.96	28.36	**28.65**
		SSIM	0.500	0.708	0.698	0.812	0.827	0.811	**0.856**
House	10	PSNR	25.72	32.69	32.42	34.80	**35.67**	34.45	35.57
		SSIM	0.634	0.804	0.830	0.858	0.907	0.878	**0.912**
	15	PSNR	23.85	31.95	31.93	34.02	34.82	34.03	**34.82**
		SSIM	0.546	0.732	0.789	0.819	0.858	0.808	**0.877**
Barbara	10	PSNR	23.69	27.62	28.41	28.47	28.41	28.33	**28.75**
		SSIM	0.602	0.788	0.798	0.812	0.799	0.802	**0.819**
	15	PSNR	22.01	26.96	27.90	28.00	27.91	27.92	**28.32**
		SSIM	0.524	0.702	0.719	0.781	0.720	0.722	**0.791**
Goldhill	10	PSNR	24.99	32.39	32.46	32.981	32.46	**33.03**	32.65
		SSIM	0.587	0.894	0.897	**0.916**	0.897	0.914	0.908
	15	PSNR	23.04	31.72	31.91	32.71	32.06	**32.79**	32.39
		SSIM	0.501	0.841	0.853	**0.890**	0.870	0.888	0.880
Peppers	10	PSNR	24.67	32.43	32.19	33.38	33.25	33.34	**33.38**
		SSIM	0.688	0.871	0.861	0.913	**0.924**	0.918	0.922
	15	PSNR	22.82	31.90	31.65	32.98	32.84	32.78	**33.01**
		SSIM	0.579	0.816	0.810	0.877	0.881	0.882	**0.891**

In Table 1, we calculate the associated $SSIM$ and $PSNR$ values for two standard deviations of the noise. The best results are shown in bold. Generally, the method of combining BTV and TV^2 outperforms the others in terms $PSNR$ and $SSIM$. On the other hand, the result obtained by the TV and BTV method exceeds the others for the *Goldhill* image in terms of $PSNR$ and $SSIM$. Indeed, we can find a better result if we change the value of the regularization parameter δ calculated automatically (see Laghrib et al. (2018b)). We can say the same thing about the *Peppers* image, in which the BTV regularization gives a better result at the level of $SSIM$ comparing to the others. However, we can deduce from the various tests that the combined TV^2 and BTV method is robust with respect to noise, comparing to the other methods. For example, we get the best value of $SSIM$ in the last image for $\sigma = 15$, while for $\sigma = 10$, the BTV method was the best.

9 Conclusion

In this paper, comparisons between the TV and high order combination models are presented, and their application for image super-resolution is tested. We present the detailed discretization process based on the finite different scheme and numerical implementation. We draw some conclusions about the advantages and disadvantages of these models using extensive comparative experiments.

Compliance with Ethical Standards

- Funding: This research was presented as a course in the West Asia Mathematical School (WAMS) : Mathematics and their interactions 2019 and was entirely funded by this school and their sponsors.

- Conflict of interest: The authors declare that they have no conflict of interest.

References

Aubert, G. & Kornprobst, P. (2006). *Mathematical problems in image processing: partial differential equations and the calculus of variations* (Vol. 147). Springer Science & Business Media.

Bergounioux, M., Piffet, L. (2010). A second-order model for image denoising. *Set-Valued and Variational Analysis, 18*(3-4), 277-306.

Chan, T., Marquina, A. & Mulet, P. (2000). High-order total variation-based image restoration. *SIAM Journal on Scientific Computing, 22*(2), 503-516.

Chambolle, A., Lions, P.L. (1997). Image recovery via total variation minimization and related problems. *Numerische Mathematik, 76*(2), 167-188.

Chambolle, A., Pock, T. (2011). A first-order primal-dual algorithm for convex problems with applications to imaging. Journal of mathematical imaging and vision, 40(1), 120-145.

Caselles, V., Chambolle, A. & Novaga, M. (2015). Total Variation in Imaging. *Handbook of Mathematical Methods in Imaging*, 1455-1499.

El Mourabit, I., El Rhabi, M., Hakim, A., Laghrib, A. & Moreau, E. (2017). A new denoising model for multi-frame super-resolution image reconstruction. *Signal Processing*, 132, 51-65.

Farsiu, S., Robinson, M.D., Elad, M. & Milanfar, P. (2004). Fast and robust multiframe super resolution. I*EEE transactions on image processing, 13*(10), 1327-1344.

Gottlieb, S., Shu, C.W. & Tadmor, E. (2001). Strong stability-preserving high-order time discretization methods. *SIAM review, 43*(1), 89-112.

Laghrib, A., Hakim, A. & Raghay, S. (2017). An iterative image super-resolution approach based on Bregman distance. *Signal Processing: Image Communication*, 58, 24-34.

Laghrib, A., Hadri, A. & Hakim, A. (2019a). An edge preserving high-order PDE for multiframe image super-resolution. *Journal of the Franklin Institute, 356*(11), 5834-5857.

Laghrib, A., Hadri, A., Hakim, A. & Raghay, S. (2019b). A new multiframe super-resolution based on nonlinear registration and a spatially weighted regularization. Information Sciences, 493, 34-56.

Laghrib, A., Ghazdali, A., Hakim, A. & Raghay, S. (2016). A multi-frame super-resolution using diffusion registration and a nonlocal variational image restoration. *Computers & Mathematics with Applications, 72*(9), 2535-2548.

Laghrib, A., Ben-Loghfyry, A., Hadri, A. & Hakim, A. (2018a). A nonconvex fractional order variational model for multi-frame image super-resolution. *Signal Processing: Image Communication*, 67, 1-11.

Laghrib, A., Hakim, A. & Raghay, S. (2015). A combined total variation and bilateral filter approach for image robust super resolution. *EURASIP Journal on Image and Video Processing*, *2015*(1), 1-10.

Laghrib, A., Ezzaki, M., El Rhabi, M., Hakim, A., Monasse, P. & Raghay, S. (2018b). Simultaneous deconvolution and denoising using a second order variational approach applied to image super resolution. *Computer Vision and Image Understanding*, 168, 50-63.

Lyaqini, S., Quafafou, M., Nachaoui, M. & Chakib, A. (2020). Supervised learning as an inverse problem based on non-smooth loss function. *Knowledge and Information Systems*, 1-20.

Papafitsoros, K., Schönlieb, C.B. (2014). A combined first and second order variational approach for image reconstruction. *Journal of Mathematical Imaging and Vision, 48*(2), 308-338.

Rudin, L.I., Osher, S. & Fatemi, E. (1992). Nonlinear total variation based noise removal algorithms. *Physica D: nonlinear phenomena, 60*(1-4), 259-268.